BIOCELL
2003, 27(2): 213-224

ISSN 0327 - 9545
PRINTED IN ARGENTINA

Apoptogenic effect of the lipophilic *o*-naphthoquinone CG 10-248 on rat hepatocytes: light and electron microscopy studies

Lidia M. Lopez*, Marta Dubin**, Patricia H. Carrizo**, Mario H. Burgos***, Amanda Pellegrino de Iraldi* and Andrés O. M. Stoppani**

* Departamento de Biología Celular y Neurociencias, Facultad de Medicina, Universidad de Buenos Aires, Argentina.
** Centro de Investigaciones Bioenergéticas, Facultad de Medicina (UBA-CONICET), Argentina.
*** Instituto de Histología y Embriología (IHEM-UNCuyo-CONICET), Mendoza, Argentina.

Keywords: Apoptosis; *o*-naphthoquinones; hepatocytes; chromatin alteration; mitochondrial swelling membrane; blebs.

ABSTRACT: CG 10-248 (3,4-dihydro-2,2-dimethyl-9-chloro-2H-naphtho[1,2b]pyran- 5,6-dione; CG-NQ), a β-lapachone analogue, modified the ultrastructure of rat hepatocytes, as demonstrated by light and electron microscopy. After 4 h incubation with 100 μM CG-NQ, the following effects were observed: (a) nuclear chromatin condensation; (b) chromatin fragmentation; (c) displacement of mitochondria, concentrated around the nucleus; (d) disruption or expansion of mitochondrial outer or inner membranes, respectively; (e) displacement and alteration of endoplasmic reticulum (rough and smooth); (f) decrease of microvilli; (g) blebbing of plasma membrane and production of apoptotic bodies formed by folding of plasma membrane fragments around mitochondria or peroxysomes; and (h) production of hydrogen peroxide. Expression of such effects varied according to hepatocyte samples and taken together strongly support an apoptotic action of CG-NQ dependent on "reactive oxygen species".

Abbreviations: CG-NQ, CG 10-248 *o*-naphthoquinone; PARP, poly(ADP- ribose)polymerase; DMFA, dimethylformamide; HRP, horseradish peroxidase.

Introduction

Lipophilic *o*-naphthoquinones exert a variety of pharmacological activities, namely, antibacterial, antifungal, trypanocidal and cytostatic effects as well as semiquinone production (Paulino *et al.,* 1994; Molina Portela *et al.,* 1996; Fernández Villamil *et al.,* 1997; Stoppani *et al.,* 2000; Dubin *et al.,* 2001, 2002). Among such quinones, β-lapachone (3,4-dihydro-2,2,dimethyl-2H-naphtho[1,2b]pyran-5,6-dione) has proven to be an effective cytostatic agent in many human tumor cell types (Dubin and Stoppani, 2000), such as promyelocytic leukemia (Li *et al.,* 2000; Planchon *et al.,* 1995, 1999; Chau *et al.,* 1998; Dolan *et al.,* 1998; Shiah *et al.,* 1999), myeloma (Li *et al.,* 2000), lymphoblastic leukemia (Frydman *et al.,* 1997), lymphoma (Manna *et al.,* 1999), prostate cancer (Li *et al.,* 1995; Planchon *et al.,* 1995; Don *et al.,* 2001), breast cancer (Wuerzberger *et al.,* 1998; Pink *et al.,* 2000b), lung carcinoma (Dolan *et al.,* 1998) and colon cancer (Huang and Pardee, 1999; Chau *et al.,* 1998; Boothman *et al.,* 1989).

Address correspondence to: Dr. Marta Dubin. Centro de Investigaciones Bioenergéticas, Facultad de Medicina, UBA, Paraguay 2155, Piso 16º, (1121) Buenos Aires, ARGENTINA. Tel/Fax: (54-11) 4508-3680; E-mail: dubin@mail.retina.ar
Received on November 19, 2002. Accepted on March 27, 2003

β-Lapachone cytotoxicity on tumor cells has been often defined as apoptosis (programmed cell death), prompted by the quinone or by its reaction products (Planchon *et al.,* 1995, 1999; Li *et al.,* 1995; Chau *et al.,* 1998; Wuerzberger *et al.,* 1998; Manna *et al.,* 1999; Huang and Pardee, 1999; Shiah *et al.,* 1999; Li *et al.,* 2000; Pink *et al.,* 2000b; Don *et al.,* 2001). Apoptosis production by β-lapachone is expressed by several cellular alterations such as (a) cell cycle inhibition; (b) nuclear fragmentation and displacement; (c) DNA laddering; (d) DNA depletion; (e) activation or inhibition of topoisomerases I and II; (f) PARP cleavage and inhibition; (g) production of reactive oxygen species (ROS); and (h) modification of cell viability.

On these grounds, β-lapachone has been proposed for clinical use (Pardee *et al.,* 2002). However, *o*-naphthoquinone cytotoxicity on tumor cells might imply "undesirable effects" for the human host. Therefore, it seemed of interest to investigate the effect of a single lipophilic *o*-naphthoquinone on a suitable biological target such as rat hepatocytes. The observations here reported are the first part of a study on the action of CG 10-248 (3,4-dihydro-9-chloro-9-2,2-dimethyl-2H-naphtho-[1,2b]pyran 5,6-dione; CG-NQ), another analogue of β-lapachone, on morphology (by light and electron microscopy) and hydrogen peroxide production by hepatocytes. CG-NQ was synthesized by Schaffner-Saba *et al.* (1984) and has been shown to exert biological activities like β-lapachone on other biological targets (Molina Portela *et al.,* 1996; Stoppani *et al.,* 2000).

Materials and Methods

Animals

Male Wistar rats (220-250 g) were used in the experiments. Animals were fed a Purina-like rat chow. Protein content of the diet was 23% and included all the essential aminoacids. A consistent light and dark cycle (12 hours) was maintained.

Chemicals

CG-NQ was obtained from Novartis (CIBA-GEIGY), Basle, Switzerland; Collagenase A from *Clostridium hystolyticum* was purchased from Boehringer Mannheim GmbH, Germany. Sucrose, dimethylformamide (DMFA), HEPES, bovine serum albumin (A-4503), EDTA, D-glucose, horseradish peroxidase (HRP), *p*-hydroxyphenylacetic acid, trizma base and Trypan blue, were purchased from Sigma Chemical Co., St. Louis, MO, USA. Other reagents were obtained from the suppliers indicated previously (Dubin *et al.,* 2001; Lopez *et al.,* 2002) and were of the highest purity available.

Isolation of hepatocytes

Hepatocytes were isolated from the liver of fed rats, which were anesthetized by intraperitoneal route with 20 μmol sodium pentobarbital (5 mg/100 g body weight). Liver cells were isolated by the method of Seglen (1973), as already described (Dubin *et al.,* 1994). Briefly, after isolation and filtration on nylon, hepatocytes were suspended in medium C (Hank's-HEPES medium) containing (mM): NaCl, 120; KCI, 5.0; $MgSO_4$, 0.5; $CaCl_2.2H_20$, 2.6; and Na_2HPO_4, 1.2; $NaHCO_3$, 4.2; HEPES, 25; saturated with CO_2/O_2 (5/95%); D-glucose, 55; bovine serum albumin, 1.5% (w/v); pH 7.4. After centrifugation at 300 rpm for 90 sec, cells were resuspended in 50 ml of medium C, allowed to settle for 10 min at 0ºC, and resuspended in the same medium to make up a suspension of approximately 5 x 10^6 hepatocytes per ml. Subsequent steps of the isolation-purification procedure were as already described (Dubin *et al.,* 1994). Cells were counted under the microscope with a hemocytometer and viability was estimated by the Trypan blue exclusion method (Moldeus *et al.,* 1978). Hepatocytes showing an initial viability greater than 95% were used for experiments.

Incubation of hepatocytes

Hepatocyte suspensions were diluted with Hank's-HEPES medium to a concentration of about 3 x 10^6 cells/ml. Duplicate samples were incubated in Erlenmeyer flasks, with CG-NQ or DMFA. Incubation was performed in a New Brunswick Gyratory Water Bath Shaker, model G76, at 37ºC and at a rate of 90 strokes/min, under carbogen atmosphere. CG-NQ or DMFA was added at zero-time, dissolving the former in DMFA. Controls received the same volume of solvent ("DMFA-samples"), whose concentration remained below 1% (v/v). Samples of incubation mixtures were taken for light or electron microscopy and for measuring H_20_2 production.

Electron and light microscopy

After incubation for 4 h, hepatocytes were centrifuged at 3,000 rpm. The pellet was fixed overnight at 4ºC with 1.5% (w/v) glutaraldehyde dissolved in 0.2 M

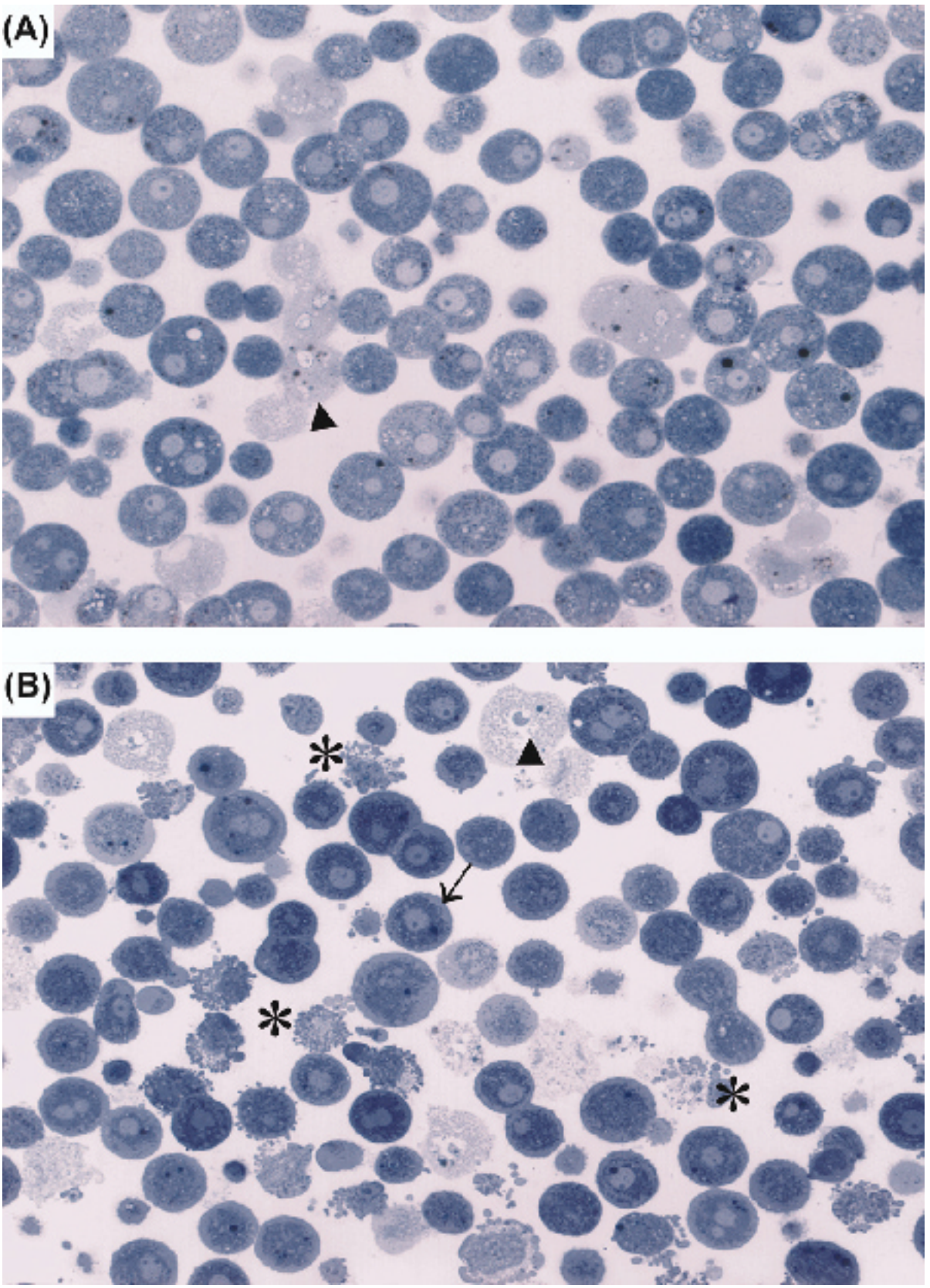

FIGURE 1. Control and CG-NQ treated hepatocyte structure (light microscopy). 400X. **A**: control normal hepatocytes, incubated with DMFA for 4 h (95% of viable hepatocytes). Black arrow head indicates necrotic hepatocytes (5% of total sample). **B**: hepatocytes incubated with 100 μM CG-NQ for 4 h (58% of cells) with preserved structure; mitochondria concentrated around the nucleus (black arrow); asterisks indicate blebs and apoptotic bodies (10% of cells). Black arrow head indicates necrotic hepatocytes (48% of cells). Light microscopy, 400X. Other conditions as in Materials and Methods.

cacodylic acid at pH 7.4-7.6. Pellets were then centrifuged at 3,000 rpm for 15 min and washed with 0.32 M sucrose in the same cacodylic acid buffer solution, in three 15-min washes. For refixation, the same buffer solution supplemented with 1.5% (w/v) osmium tetroxide was applied for two hours at 4ºC. After briefly washing with distilled water, pellets were resuspended for 2 h in 2% (w/v) uranyl acetate and immediately dehydrated for pre-embedding. After embedding, ultrathin sections were stained with 2% (w/v) uranyl acetate in water and afterwards with Reynolds solution. Microphotographs were obtained by means of a C10 Zeiss Electron Microscope using Kodak 4489 Films. For light microscopy, sections were then stained with 0.5% toluidine blue and 0.1% cresyl blue. Observations were performed with an Olympus BX50 microscope equipped with a COOL-SNAP-PRO digital camera, objective 40X.

Hydrogen peroxide production was measured by *p*-hydroxylphenyl acetate peroxidation in the presence of HRP (Hyslop and Sklar, 1984). The reaction mixture contained 3 x 10^6 hepatocytes/ml in Hank's-HEPES medium, pH 7.4, 100 μM CG-NQ,12 U/ml horseradish peroxidase (HRP), and 2.5 mM *p*-hydroxyphenyl acetic acid. Fluorescence was measured at 317 and 414 nm (excitation and emission, respectively), using an SRSLM Aminco spectrofluorometer.

Results

CG-NQ treatment of hepatocytes produced diverse alterations in cell structure, including the nuclear chromatin, mitochondrion, endoplasmic reticulum and plasma membrane. Such alterations were not equally distributed in all hepatocytes and, therefore, in order to provide a full picture of CG-NQ-induced cell damage, presentation of a number of dissimilar typical hepatocyte samples seems justified. These samples were obtained from similarly incubated hepatocytes (4 h incubation), with 100 μM CG-NQ and the corresponding solvent (DMFA) and are thus strictly comparable. The number of modified hepatocytes was determined throughout and its relative proportion (%) was expressed as a fraction of the total number of hepatocytes examined in each sample (at least 50 cells).

Structural alterations in treated hepatocytes, incubated with 100 μM CGNQ for 4 h, as compared with the corresponding control cells (light microscopy), are depicted in Figure 1. Most hepatocytes (58%) showed mitochondria displaced towards the cell nucleus, 32% presented plasma membrane blebbing and 10% exhibited necrosis. At variance with these results, control hepatocytes displayed preserved structure, allowance made for those presenting necrosis (5%).

Figure 2 depicts the preserved ultrastructure of control hepatocytes (electron microscopy), while the inset shows the amplified, preserved ultrastructure of mitochondria and of the endoplasmic reticulum (rough and smooth) in the same hepatocytes.

Figure 3 shows the ultrastructure of (a) CG-NQ treated hepatocyte sample. In the main figure, the more significant alterations were (a) mitochondrial concentration around the nucleus; (b) endoplasmic reticulum (rough and smooth) moved towards the plasma membrane; (c) microvilli scarcity; and (d) incipient blebbing of the plasma membrane. Figure A provides an amplified view of the mitochondrion with preserved membranes and a peroxysome, while Figure B shows the endoplasmic reticulum with expanded cisternae and reduced number of ribosomes.

Figure 4 presents a more remarkable picture of hepatocyte damage by CG-NQ. Thus, Figure 4A, depicts a single binucleated hepatocyte with condensed chromatin, bound to the nuclear membrane; most mitochondria were swollen and the plasma membrane showed abundant blebs. In the same picture appear, however, two preserved hepatocytes. Figure 4B includes hepatocytes with their nuclei displaced towards the plasma membrane, abundant aggregated chromatin, swollen mitochondria, vacuolized cytosol and blebs.

Figures 5A-C also illustrate extensive structural damage in CG-NQ-treated hepatocytes. There was cell disintegration with nuclear fragmentation, and large membrane blebs, apoptotic bodies, consisting in pieces of cytosol wrapped in the plasma membrane and containing organelles (mitochondria and endoplasmic reticulum (rough and smooth), as well as swollen mitochondria with condensed matrix. Figure 5D shows the disruption of outer mitochondrial membranes, fragments of which remain preserved. The mitochondrial inner membrane is expanded but preserved, while the matrix appears swollen. Figure E again shows nuclear fragmentation and mitochondrial matrix condensation, that appears dark and small. In other hepatocyte samples, abundant mitochondria were either swollen or condensed, as in Figure 5E.

Hydrogen peroxide production resulting from superoxide dismutation immediately followed CG-NQ addition to hepatocytes and its concentration, increased progressively to reach an effective concentration after 60 min of incubation, which implies possible cytotoxic effects in the subsequent incubation period. Hydrogen

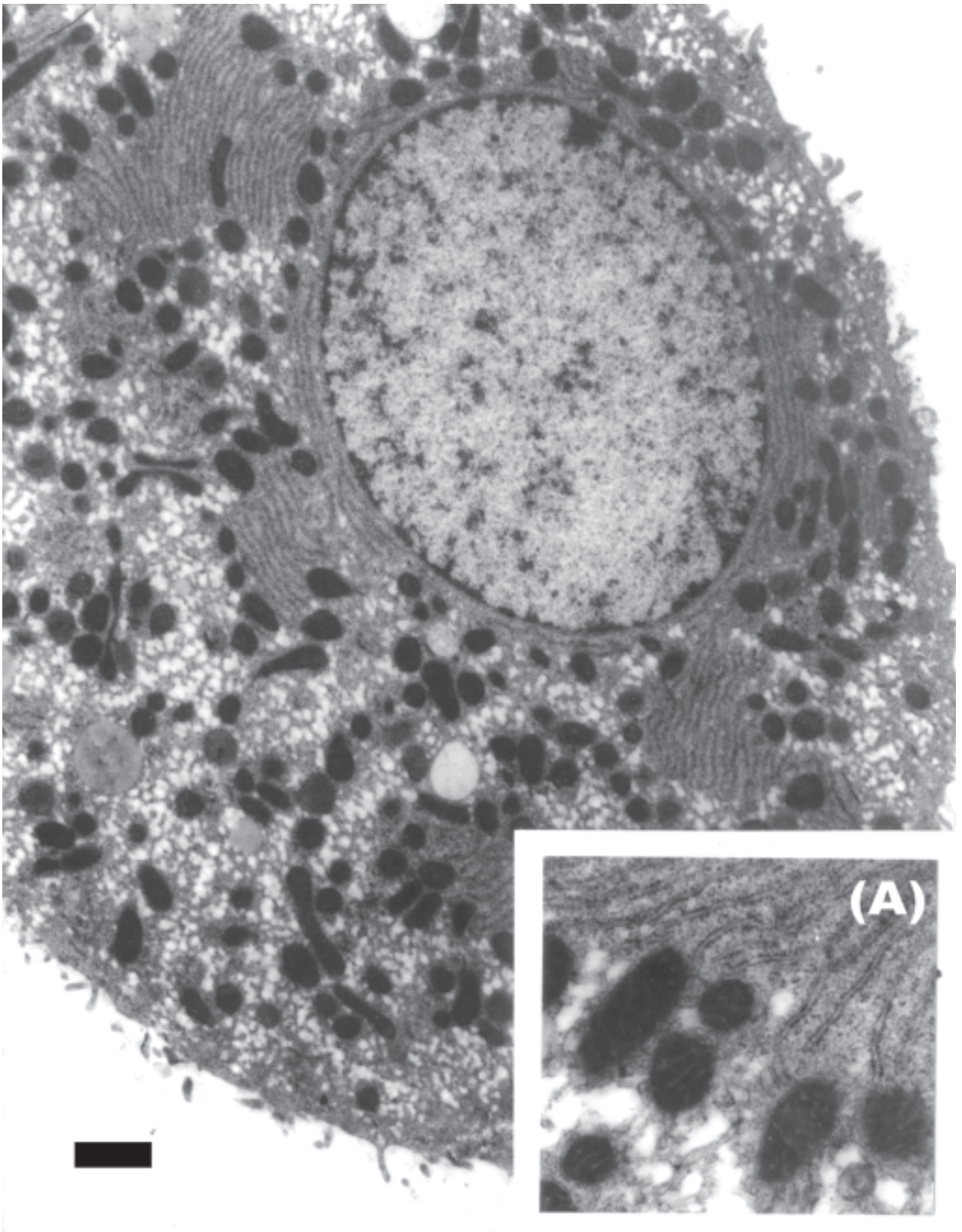

FIGURE 2. Control normal hepatocytes ultrastructure (electron microscopy). Main figure: hepatocytes incubated with DFMA for 4 h with preserved nucleus, cytoplasm and microvilli. 3,150X. Bar: 1 cm ≡ 1.0 μm. Inset: enlarged. **A**: mitochondria with dense matrix and normal cristae, preserved plasma membrane. Preserved endoplasmic reticulum (rough and smooth). 10,000X. Bar: 1 cm ≡ 0.4 μm. Other conditions as in Materials and Methods.

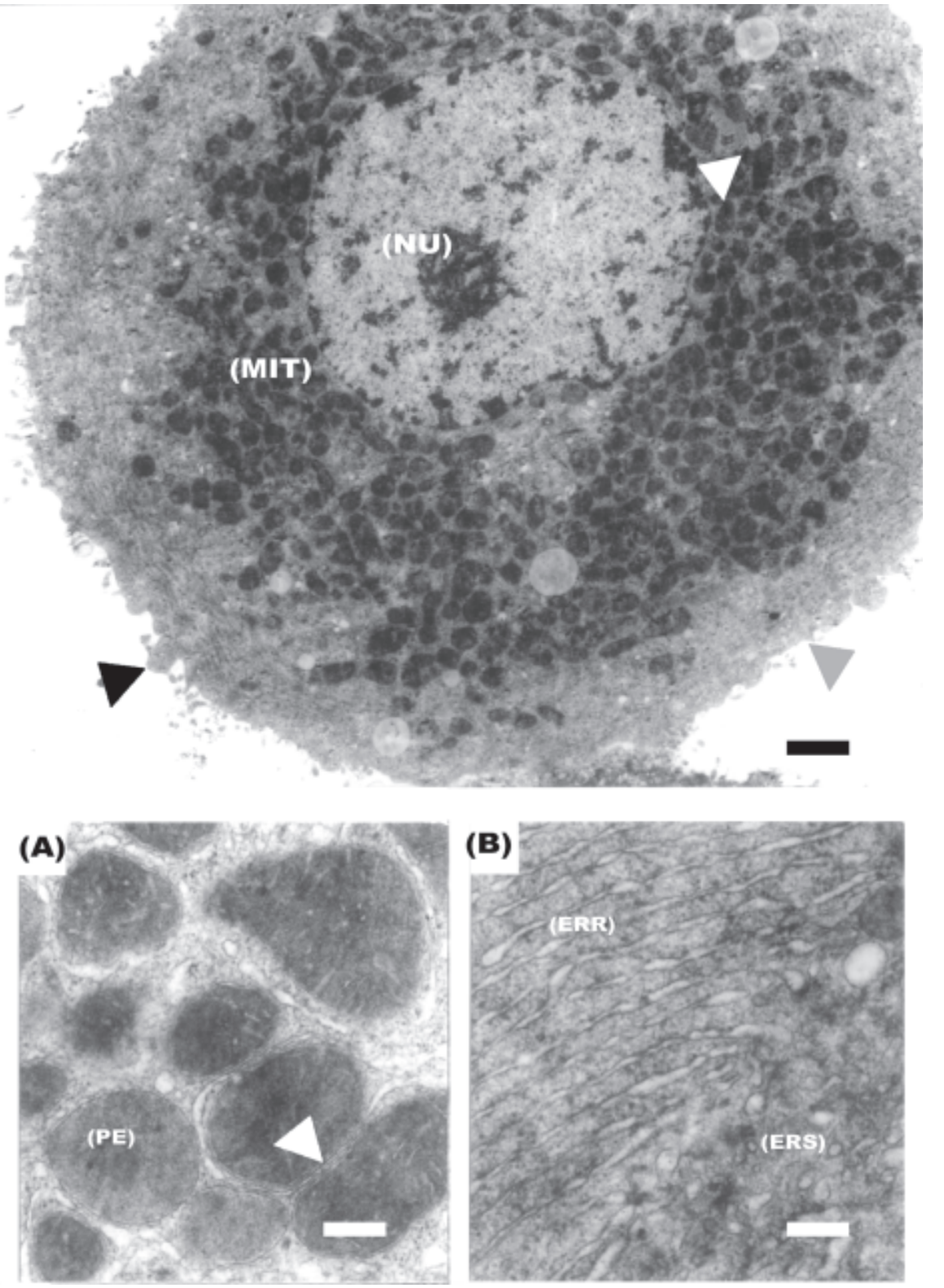

FIGURE 3. CG-NQ treated hepatocyte ultrastructure (electron microscopy). Sample representing 58% of hepatocytes. Main figure: scattered nuclear chromatin (white arrow head); preserved nucleolus (NU); mitochondria concentrated around the nucleus (MIT); endoplasmic reticulum (rough and smooth) displaced towards the plasma membrane; scarce microvilli (gray arrow head); incipient blebbing (black arrow head). 2,500X. Bar: 1 cm ≡ 3.2 μm. **A:** preserved mitochondrial membranes (white arrow head), preserved peroxysome (PE). 12,500X. Bar: 1 cm ≡ 0.22 μm. **B:** rough and smooth (ERR, ERS) endoplasmic reticulum with expanded cisternae and scarce ribosomes. 12,500X. Bar: 1 cm ≡ 0.22 μm. Other conditions as in Materials and Methods.

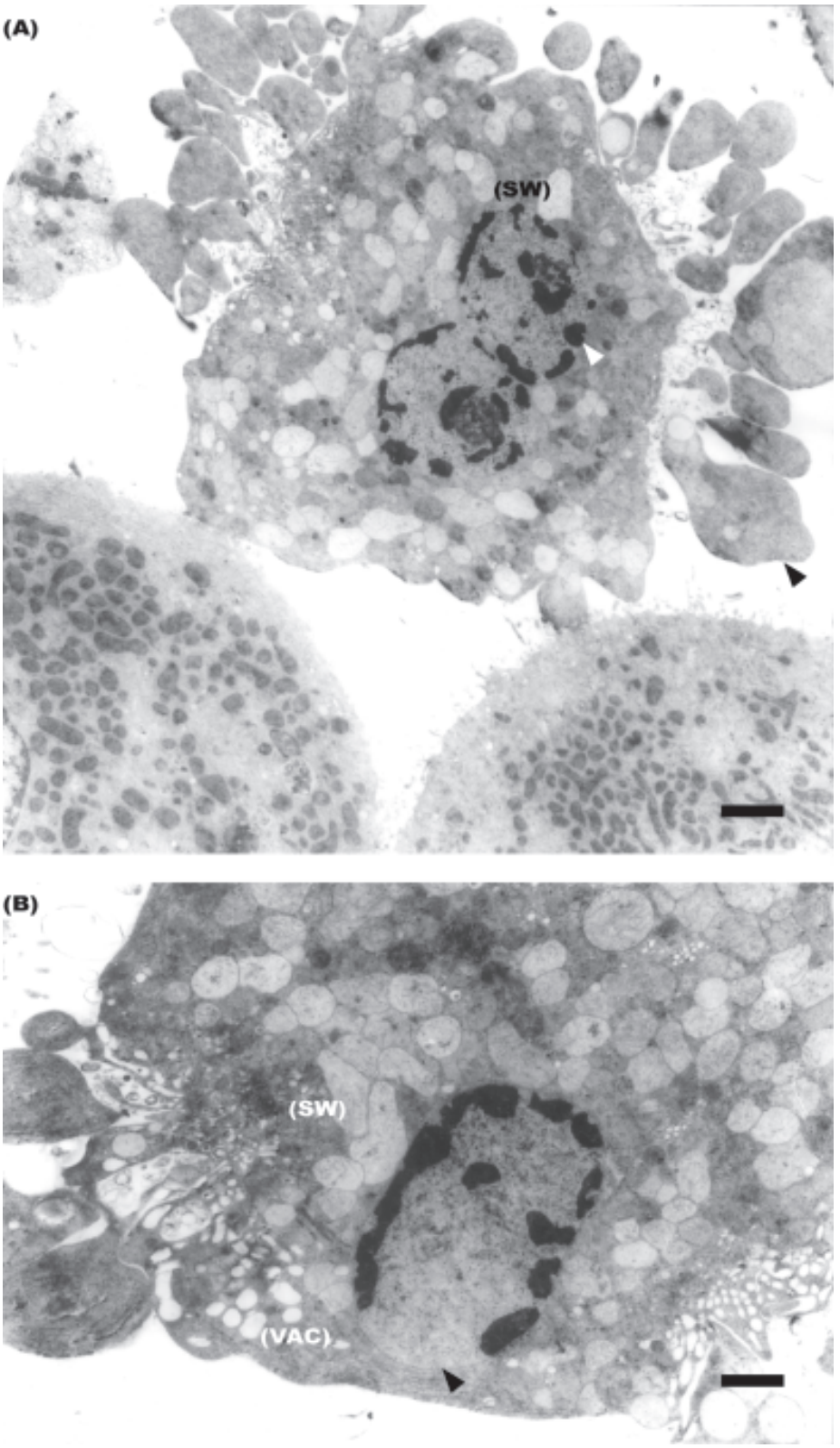

FIGURE 4. CG-NQ-treated hepatocyte ultrastructure (electron microscopy). Sample representative of 32% of cells. **A**: binucleated hepatocyte with condensed chromatin, approaching the nuclear membrane (white arrow head); abundant swollen mitochondria (SW); plasma membrane showing blebs (black arrow head). In the same figure, two preserved hepatocytes. 2,500X. Bar: 1 cm ≡ 2.0 μm. **B**: similar sample showing nucleus displaced towards the plasma membrane; chromatin largely condensed near the non-modified nuclear membrane (black arrow); vacuoles (VAC); abundant swollen mitochondria (SW); plasma membrane showing blebs. 3,150X. Bar: 1 cm ≡ 1.4 μm. Other conditions as in Materials and Methods.

peroxide production was confirmed by adding azide to the hepatocyte suspension. Azide is a specific inhibitor of catalase, the enzyme that decomposes hydrogen peroxide in hepatocytes, thus exerting an antioxidant action. In close agreement with its specific function, azide increased hydrogen peroxide production by hepatocytes, its effect being remarkable during the first 15 or 30 min of incubation, as compared with control values ($p \leq 0.005$ or 0.01) for 15 or 30 min incubation time, respectively.

Discussion

The observations described here indicate that, after 4 h incubation of hepatocytes with CG-NQ, significant structural changes occurred. These effects were quite compatible with the apoptotic action of a similar *o*-naphthoquinone, β-lapachone, in tumor cells, as described in the literature. The structural changes produced by CG-NQ in hepatocytes were not homogenous (Figs. 1-5), varying in extent and location. Since hepatocyte samples were all taken from the same incubation mixture at the same incubation time, which was adequate for apoptosis in tumor cells, it must be concluded that CG-NQ action was affected by metabolic peculiarities inherent to cell physiology.

Among the hepatocyte alterations caused by CG-NQ, those of the nucleus seemed particularly crucial to qualify quinone-induced damage as apoptosis. In fact, chromatin alterations are characteristic of β-lapachone induced apoptosis in tumor cells (Planchon *et al.,* 1995, 1999; Li *et al.,* 1995; Wuerzberger *et al.,* 1998; Chau *et al.,* 1998; Shiah *et al.,* 1999; Pink *et al.,* 2000b). These alterations correlate with DNA repair inhibition by β-lapachone both in tumor (Boothman *et al*., 1989) and *Trypanosoma cruzi* cells (Goijman and Stoppani, 1985). The effects of β-lapachone include DNA depletion, condensation, laddering and chromatin fragmentation, as described in tumor cells. Similar effects were produced by CG-NQ in hepatocytes (Figs. 3-5). These processes may well represent modification of enzymes responsible for DNA repair such as topoisomerases (Boothman *et al.,* 1989; Degrassi *et al.,* 1993; Li *et al.,* 1995; Frydman *et al.,* 1997; Pink *et al.,* 2000a; Shiah *et al.,* 1999) and PARP (Chau *et al.,* 1998; Vanni *et al.,* 1998; Pink *et al.,* 2000a; Don *et al.,* 2001; Fernández Villamil *et al.,* 2001). Taking into account the foregoing, CG-NQ effect on hepatocyte DNA may be explained as a result of (a) direct enzyme inhibition by CG-NQ (e.g. topoisomerases), or (b) by the action of redox activated CG-NQ products including reactive oxygen species (ROS). These reaction products may activate a nuclear signal (e.g. DNA damage) (Walles, 1992) which triggers down-stream apoptosis (Pink *et al.,* 2000b). Damaged cells would then become sensitive to topoisomerase inhibition by the quinone. In addition to these effects, the quinones may inactivate PARP (Pink *et al.,* 2000a; Li *et al.,* 2000; Fernández Villamil *et al.,* 2001) which is involved in DNA repair. The mechanism of PARP inactivation may result from the activation of caspases by the quinone or its reactive derivatives (Planchon *et al.,* 1999; Li *et al.,* 2000) or by a direct action of the quinone (Fernández Villamil *et al.,* 2001).

In close agreement with previous observations using isolated rat liver mitochondria (Lopez *et al.,* 2002), CG-NQ produced significant mitochondrial alterations, including disruption or disappearance of the outer membrane and matrix swelling (Figs. 4B, 5D). Mitochondrial alterations were closely related to apoptosis (Zamzami *et al.,* 1995; Vander Heiden *et al.,* 1997). Membrane disruption may depend on inner membrane depolarization by the quinone (Hacker, 1999). Consistent effects were observed with isolated mitochondria incubated with CG-NQ using rhodamine 123 as elec-

FIGURE 5. CG-NQ-treated hepatocytes ultrastructure (electron microscopy). **A**: hepatocytes showing variable degrees of disintegration, with large blebs separating from the cell membrane and producing apoptotic bodies (black arrow head) 3,150X. Bar: 1 cm / 2.11 μm. **B**: Apoptotic body showing swollen and condensed mitochondria and endoplasmic reticulum (rough and smooth) surrounded by plasma membrane 12,500X. Bar: 1 cm ≡ 0.5 μm. **C**: showing nucleus fragmented at different sites (black arrow head); abundant swollen and condensed mitochondria; plasma membrane with blebs. 3,150X. Bar: 1 cm ≡ 2.1 μm. **D**: same hepatocyte sample showing partial disruption of mitochondrial outer membrane; preserved inner membrane (one black arrow head) with swollen matrix. Two white arrow heads indicate partially preserved outer mitochondrial membrane. Li, lipid drop. 12,500X. Bar: 1 cm ≡ 0.3 μm. **E**: fragmented nucleus (white arrow head); MITCON mitochondria with preserved membranes and condensed matrix; LI, lysosomes. 12,500X. Bar: 1 cm ≡ 0.5 μm. Other conditions as in Materials and Methods.

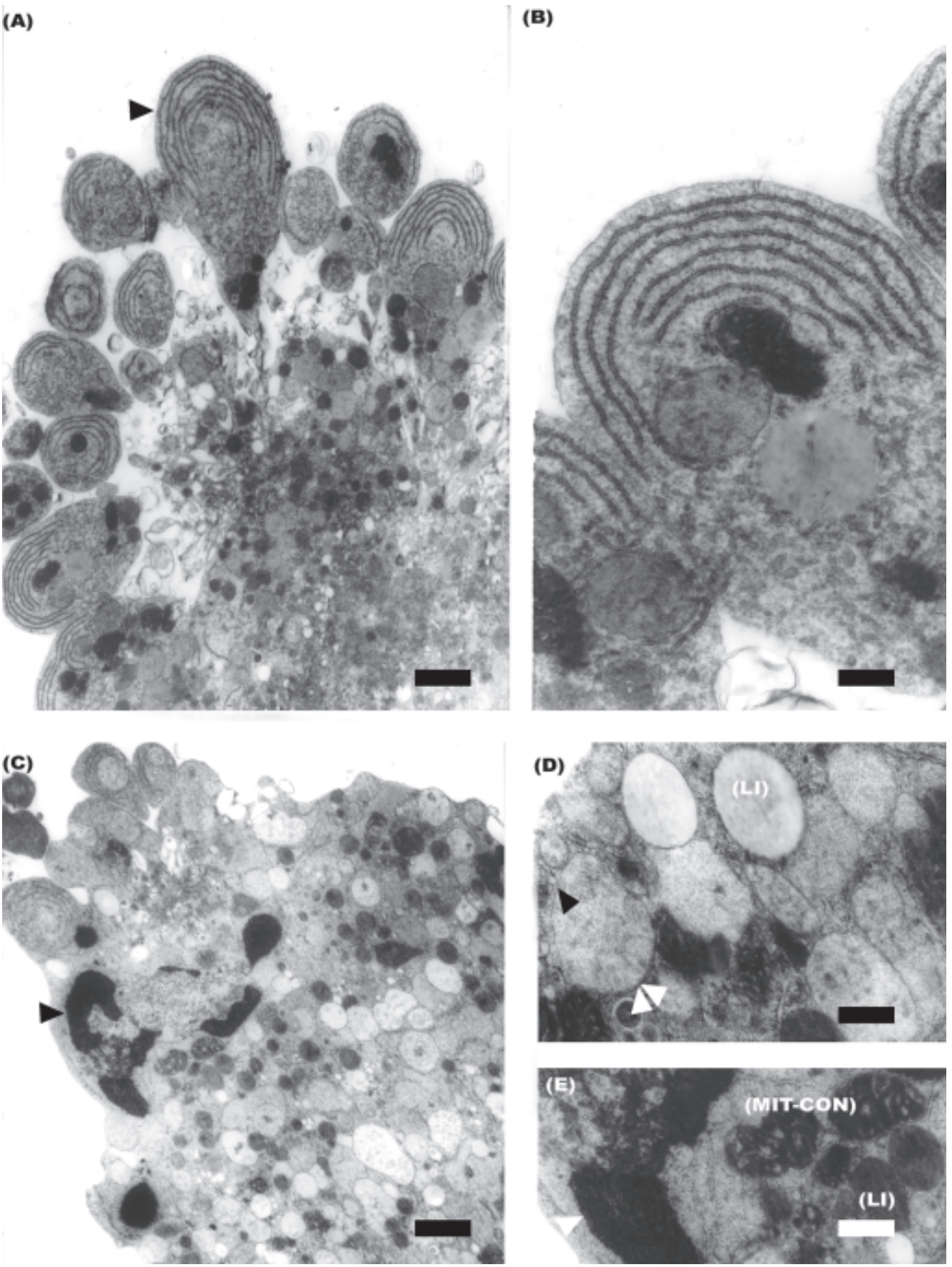
(A)
(B)
(C)
(D)
(LI)
(E)
(MIT-CON)
(LI)

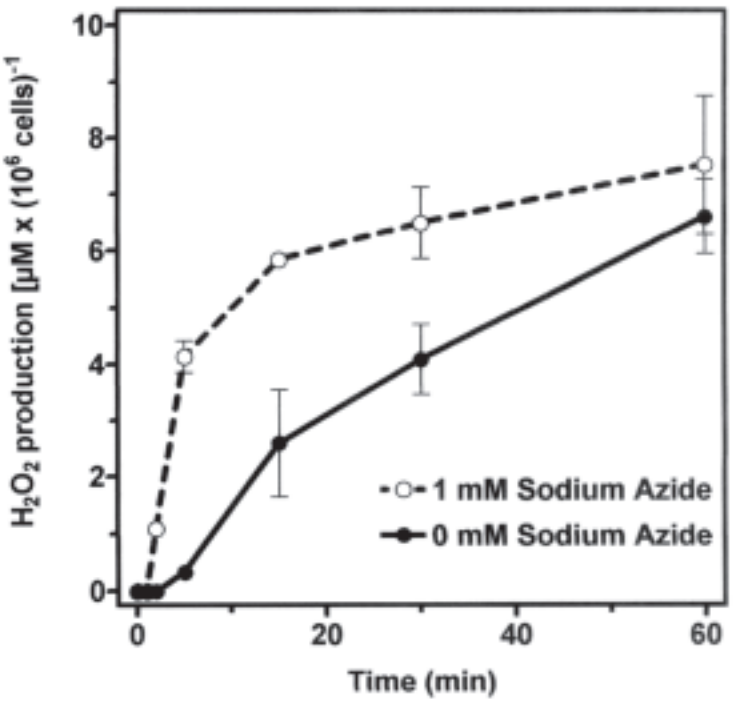

FIGURE 6. Effect of CG-NQ on H_20_2 production by hepatocytes. The reaction medium contained 3 x 10^6/ml cells. Sodium azide (AZ), control without sodium azide (C). Values are means ± S.E.M. of three duplicate independent measurements. Other conditions as in Materials and Methods.

trochemical potential indicator (data not shown). In addition to the alterations of mitochondria structure reported here, CG-NQ could also affect mitochondrial functions, specially ATP production, F_0F_1-ATPase activity and ion translocation (Lopez *et al.,* 2002). CG-NQ dependent mitochondrial swelling would contribute to apoptosis (Vander Heiden *et al.,* 1997) since it would lead to opening of the mitochondrial permeability pore and the release of cytochrome c, which in turn would contribute to apoptogenesis (Kroemer, 1999; Zamzami *et al.,* 1996). Another interesting action of CG-NQ was the appearance of vacuoles in hepatocyte cytoplasm (Fig. 4B) and the modification of the endoplasmic reticulum, specially its displacement towards the plasma membrane. Vacuole formation is typical of apoptotic cells but the mechanism of vacuolization is not clear (Fearnhead *et al.,* 1995; Henics and Wheatley, 1999).

A peculiar feature of CG-NQ action on hepatocytes was the modification of the plasma membrane (Fig. 1-5). Blebs are protrusions of the plasma membrane that may contain other cell structures such as mitochondria and peroxysomes, constituting the apoptotic body. Another alteration of the plasma membrane was the partial or total disappearance of microvilli. As regards blebbing, studies with cytochalasin D indicate that microfilament structure must be re-ordered to produce blebs and therefore blebbing implies a modification of the cytoskeleton (Thör *et al.,* 1988; Mirabelli *et al.,* 1988; Kondo *et al.,* 1997; Huot *et al.,* 1998; Chen *et al.,* 2000). Hepatocyte modification by naphthoquinones, such as menadione, depends on cytoskeleton modification (active polymerization inhibition) (Thör *et al.,* 1988). Blebbing in hepatocytes is associated to GSH depletion, an effect that occurs after incubation of hepatocytes with lipophilic *o*-naphthoquinones (Dubin *et al.,* 2002). Loss of microvilli is related to caspase activation, an effect frequently observed after treatment of cells with "reactive oxygen species" generators.

To sum, own results indicate that CG-NQ, a lipophilic *o*-naphthoquinone, at 100 µM concentration, is capable of inducing apoptosis in rat hepatocytes. These effects raise the question whether similar changes would occur in organisms treated with this and similar *o*-naphthoquinones such as β-lapachone, which are potential cytostatic agents (Pardee *et al.,* 2002).

Acknowledgments

This work was supported by Grants from the University of Buenos Aires and Roemmers Foundation. P. Corazza, M.A. Verón and S. Del Valle lent able technical assistance.

References

Boothman DA, Trask DK, Pardee AB (1989). *Inhibition of potentially lethal DNA damage repair in human tumor cells by ß-lapachone, an activator of topoisomerase I*. Cancer Res 49: 605-612.

Chau Y-P, Shiah S-G, Con M-J, Kuo M-L (1998). *Involvement of hydrogen peroxide in topoisomerase inhibitor ß-lapachone-induced apoptosis and differentiation in human leukemia cells*. Free Radical Biol Med 24: 660-670.

Chen HW, Chlang T, Wang CY, Lii CK (2000). *Inhibition of tert-butyl hydroperoxide-induced cell membrane bleb formation by alpha-tocopherol and glutathione*. Food Chem Toxicol 38: 1089-1096.

Degrassi F, De Salvia R, Berghella L (1993). *The production of chromosomal alterations by ß-lapachone, an activator of topoisomerase I*. Mutat Res 288: 263-267.

Dolan ME, Frydman B, Thompson CB, Diamond AM, Garbiras BJ, Safa AR, Beck WT, Marton LJ (1998). *Effect of 1,2-naphthoquinones on human tumor cell growth and lack of cross-resistance with other anticancer agents*. Anti-cancer Drugs 9: 437-448.

Don M-J, Chang Y-H, Chen K-K, Ho L-K, Chau Y-P (2001). *Induction of CDK inhibitors (p21WAF1 and p27Kip1) and Bak in the ß-lapachone induced apoptosis of human prostate cancer cells*. Mol Pharmacol 59: 784-794.

Dubin M, Stoppani AOM (2000). *Muerte celular programada y apoptosis*. Medicina 60: 375-386.

Dubin M, Carrizo PH, Biscardi AM, Fernandez Villamil SH, Stoppani AOM (1994). *Effect of 5-nitroindole on adenylate energy charge, oxidative phosphorylation and lipid peroxidation in rat hepatocytes*. Biochem Pharmacol 48: 1483-1492.

Dubin M, Fernández Villamil SH, Stoppani AOM (2001). *Citotoxicidad de la ß-lapachona, una o-naftoquinona con posibles usos terapéuticos*. Medicina-Buenos Aires 61: 343-350.

Dubin M, Fernández Villamil SH, De Witte N, Carrizo P, Molina Portela MP, Stoppani AOM (2002). *Possible cytotoxic effects of lipophilic o-naphthoquinones in isolated rat hepatocytes. Protective mechanisms*. In: Sixth International Symposium on Predictive Oncology and Intervention Strategies, H.E. Nieburgs, Ed. Elsevier Science Inc, p. 179.

Fearnhead HO, Dinsdale D, Cohen GM (1995). *An interleukin-1ß-converting enzyme-like protease is a common mediator of apoptosis in thymocytes*. FEBS Lett 375: 283-288.

Fernández Villamil SH, Dubin M, Molina Portela MP, Perissinotti LJ, Brusa MA, Stoppani AOM (1997). *Semiquinone production by lipophilic o-naphthoquinones*. Redox Report 3: 245-252.

Fernández Villamil SH, Podesta D, Molina Portela MP, Stoppani AOM (2001). *Characterization of poly(ADP-ribose)polymerase from Crithidia fasciculata: enzyme inhibition by ß-lapachone*. Mol Biochem Parasitol 115: 249-256.

Frydman B, Marton LJ, Sun JS, Neder K, Witiak DT, Liu AA, Wang H-M, Mao Y, Wu H-Y, Sanders MM, Liu LF (1997). *Induction of DNA topoisomerase II-mediated DNA cleavage by ß-lapachone and related naphthoquinones*. Cancer Res 57: 620-627.

Goijman SG, Stoppani AOM (1985). *Effects of ß-lapachone, a peroxide-generating quinone, on macromolecule synthesis and degradation in Trypanosoma cruzi*. Arch Biochem Biophys 240: 273-280.

Hacker G (1999). *The morphology of apoptosis*. Cell Tissue Res 301: 283-288.

Henics T, Wheatley DN (1999). *Cytoplasmic vacuolation, adaptation and cell death, a view on new perspectives and features*. Bio Cell 91: 485-498.

Huang L, Pardee AB (1999). *ß-lapachone induces cell cycle arrest and apoptosis in human colon cancer cells*. Mol Med 5: 711-720.

Huot J, Houle F, Rousseau S, Deschesness RG, Shah GM, Landry J (1998). *SAPK2/p38-dependent F-actin reorganization regulates early membrane blebbing during stress-induced apoptosis*. J Cell Biol 143: 1361-1373.

Hyslop PA, Sklar LA (1984). *A quantitative fluorimetric assay for the determination of oxidant production by polymorphonuclear leukocytes: its use in the simultaneous fluorimetric assay of cellular activation processes*. Arch Biochem Biophys 141: 380-386.

Kondo F, Takeuchi K, Doi Y, Yonemura S, Nagata S, Tsukita D (1997). *ERM (ezrin/radixin/moesin)-baswd molecular mechanism of microvillar breakdown at an early stage of apoptosis*. J Cell Biol 139: 749-758.

Kroemer G (1999). *Mitochondrial control of apoptosis: an overview*. In: Mitochondria and Cell Death, G.C. Brown, D.G. Nicholls, C.E. Cooper, Eds. Portland Press, pp. 1-15.

Li CJ, Wang C, Pardee AB (1995). *Induction of apoptosis by ß-lapachone in human prostate cancer cells*. Cancer Res 55: 3712-3715.

Li Y, Li CJ, Yu D, Pardee AB (2000). *Potent induction of apoptosis by ß-lapachone in human multiple myeloma cell lines and patient cells*. Mol Med 6: 1008-1015.

López LM, Pellegrino de Iraldi A, Carrizo PH, Dubin M, Stoppani AOM (2002). *Effect of the lipophilic o-naphthoquinone CG 10-248 on rat liver mitochondria structure and function*. Biocell 26: 237-245.

Manna S, Gad YP, Mukhopadhyay A, Aggarwal BB (1999). *Suppression of tumor necrosis factor-activated nuclear transcription factor-kB, activator protein-1, c-Jun N-terminal kinase, and apoptosis by ß-lapachone*. Biochem Pharmacol 57: 763-774.

Mirabelli F, Salis A, Marinoni V, Finardi G, Bellomo G, Thör H, Orrenius DS (1988). *Menadione-induced bleb formation in hepatocytes is associated with the oxidation of thiol groups in actin*. Arch Biochem Biophys 264: 261-269.

Moldeus P, Högberg J, Orrenius S (1978). *Isolation and use of liver cells*. Methods Enzymol 52: 60-71.

Molina Portela MP, Fernández Villamil SH, Perissinotti LJ, Stoppani AOM (1996). *Redox cycling of o-naphthoquinones in trypanosomatids. Superoxide and hydrogen peroxide production*. Biochem Pharmacol 52: 1875-1882.

Pardee AB, Li YZ, Li CJ (2002). *Cancer therapy with beta-lapachone*. Curr Cancer Drug Targets 2: 227-242.

Paulino M, Hansz M, Hikichi N, Tabares G, Molina Portela MP, Fernandez Villamil SH, Sreider CM, Stoppani AOM (1994). *Propiedades electrónicas y actividad redox de naftoquinonas*. An Asoc Quim Argent 82: 371-389.

Pink JJ, Planchon SM, Tagliarino C, Varnes ME, Siegel D, Boothman DA (2000a). *NAD(P)H: Quinone oxidoreductase activity is the principal determinant of ß-lapachone cytotoxicity*. J Biol Chem 275: 5416-5424.

Pink JJ, Wuerzberger-Davis S, Tagliarino C, Planchon SM, Yang XH, Froelich CJ, Boothman DA (2000b). *Activation of a cysteine protease in MCF-7 and T47D breast cancer cells during ß-lapachone-mediated apoptosis*. Exp Cell Res 255: 144-155.

Planchon SM, Wuerzberger S, Frydman B, Witiak DT, Hutson P, Church DR, Wilding G, Boothman DA (1995). *ß-lapachone-mediated apoptosis in human promyelocytic leukemia (HL-60) and human prostate cancer cells: A p53-independent response*. Cancer Res 55: 3706-3711.

Planchon SM, Wuerzberger-Davis SM, Pink JJ, Robertson KA, Bornmann WG, Boothman DA (1999). *Bcl-2 protects against ß-lapachone-mediated caspase 3 activation and apoptosis in human myeloid leukemia (HL-60) cells*. Oncol Rep 6: 485-492.

Schaffner-Sabba K, Schmidt-Ruppin KH, Wehrli W, Schuerch AR, Wasley JWF (1984). *ß-lapachone: synthesis of derivatives and activities in tumor models*. J Med Chem 27: 990-994.

Seglen PO (1973). *Preparation of rat liver cells. III. Enzymatic requirements for tissue dispersion*. Exp Cell Res 82: 391-398.

Shiah S-G, Chuang S-E, Chau Y-P, Shen S-C, Kuo M-L (1999). *Activation of c-Jun NH_2-terminal kinase and subsequent CPP32/Yama during topoisomerase inhibitor ß-lapachone-induced apoptosis through an oxidation dependent pathway*. Cancer Res 59: 391-398.

Stoppani AOM, Goijman S, Dubin M, Fernández Villamil SH, Molina Portela MP, Biscardi AM, Paulino M (2000). *Cytotoxicity of lipophilic o-naphthoquinones: structure-activity relationship*. Trends Comp Biochem Physiol 7: 1-16.

Thör H, Mirabelli F, Salis A, Cohen GM, Bellomo G, Orrenius S (1988). *Alterations in hepatocyte cytoskeleton caused by redox cycling and alkylating quinones*. Arch Biochem Biophys 266: 397-407.

Vander Heiden MG, Chandel NS, Williamson EK, Schumacker PT, Thompson CB (1997). *Bcl-x(L) regulates the membrane potential and volume homeostasis of mitochondria*. Cell 91: 627-637.

Vanni A, Fiore M, De Salvia R, Cundari E, Ricordy R, Ceccarelli R, Degrassi F (1998). *DNA damage and cytotoxicity induced by ß-lapachone: relation to poly(ADP-ribose)polymerase inhibition*. Mutat Res 401: 55-63.

Walles S (1992). *Mechanism of DNA damage induced in rat hepatocytes by quinones*. Cancer Res 63: 47-52.

Wuerzberger SM, Pink JJ, Planchon SM, Byers KL, Bornmann WG, Bothman DA (1998). *Induction of apoptosis in MCF-7:WS8 cancer cells by ß-lapachone*. Cancer Res 58: 1876-1885.

Zamzami N, Marchetti P, Castedo M, Decaudin D, Macho A, Hirsch T, Susin SA, Petit PX, Mignotte B, Kroemer G (1995). *Sequential reduction of mitochondrial transmembrane potential and generation of reactive oxygen species in early programmed cell death*. J Exp Med 182: 367-377.

Zamzami N, Marchetti P, Castedo M, Hirsch T, Susin SA, Masse B, Kroemer G (1996). *Inhibitors of permeability transition interfere with the disruption of the mitochondrial transmembrane potential during apoptosis*. FEBS Lett 384: 53-57.